Available online at www.sciencedirect.com
ScienceDirect
International Journal of Thermal Sciences 46 (2007) 637–648
International Journal of Thermal Sciences
www.elsevier.com/locate/ijts

Numerical simulation of double diffusive laminar mixed convection in a horizontal annulus with hot, solutal and rotating inner cylinder

Mohamed A. Teamah

Mechanical Engineering Department, Alexandria University, Alexandria, Egypt

Received 6 July 2006; received in revised form 12 August 2006; accepted 10 September 2006

Available online 9 October 2006

Abstract

A numerical investigation of double-diffusive laminar mixed convection within a two-dimensional, horizontal annulus has been carried out. The inner cylinder was considered to rotate in an anti-clockwise direction to introduce the forced convection effect. In addition, the solutal and thermal buoyancy forces are sustained by maintaining the inner and outer cylinders at uniform temperatures and concentrations, but their values for the inner are higher than the outer. The laminar flow regime is considered under steady state conditions. Moreover, the transport equations for continuity, momentum, energy and mass transfer are solved using the Patankar–Spalding technique. The streamlines, isotherms and isoconcentrations as well as both local and average Nusselt and Sherwood numbers were studied. The study covers a wide range for $10^2 \leqslant Ra_T \leqslant 10^6$, $0.1 \leqslant Le \leqslant 10$ and $-20 \leqslant N \leqslant 20$. Through this investigation, the following parameters are kept constant: Prandtl number at 0.7, the rotational Reynolds number at 100 and the radius ratio at 0.5. The predicted results for both average Nusselt and Sherwood numbers were correlated in terms of Lewis number, thermal Rayleigh number and buoyancy ratio. A comparison was made with the published results and a good agreement was found.

Keywords: Double-diffusive flow; Heat and mass transfer; Rotating annulus; Mixed convection; Two-dimensional; Numerical simulation

1. Introduction

Double-diffusive convection is referred to the problems where the fluid flow is induced by the simultaneous presence of two diffusive components. These are the difference in temperatures and concentrations. A substantial amount of research has been reported on double-diffusive convection in confined spaces due to its many engineering and technology applications. Such as, the technologies involved in the chemical vapor deposition processes for the semiconductor device fabrications. Also, the migration of impurities in non-isothermal material processing applications has motivated many researchers in exploring the characteristics of the associated species and energy transport processes. The effect of forced flow in a double-diffusive convection has been considered in natural phenomena as atmospheric and oceanic flows. Also, these phenomena appear in many engineering applications. The migration of the species is known to be sensitive to the magnitude of rotational speed, which is a crucial parameter in drying technologies, printing and crystal growth applications. Other technologies including melting and solidification processes in rotating furnace are likely candidates for such applications. In addition, the flow and heat transfer characteristics under the simultaneous effect of temperature and concentration gradients as well as the centrifugal forces are defined by the mixed convection. In general, both thermal and solutal Grashof numbers as well as the rotational Reynolds number represent these effects.

Early studies of the combined heat and mass transfer in rectangular enclosures were reported by Hu and EL-Wakil [1], Ostrach [2–4] has pointed out that various convection modes can emerge based on the orientations of the temperature and concentration gradients. For a vertical annulus, Ship et al. [5] conducted a numerical study for steady laminar double-diffusive natural convection within a vertically mounted closed annulus with constant temperature and mass species differences imposed across the vertical walls. Their results showed that the buoyancy ratio was the primary parameter that defined the flow

E-mail address: mteamah@yahoo.com.

1290-0729/$ – see front matter
doi:10.1016/j.ijthermalsci.2006.09.002

Nomenclature

b	annulus gab width, $b = (r_o - r_i)$ ..... m
C	vapour concentration
C^*	dimensionless vapour concentration, $C^* = (C - C_o)/(C_i - C_o)$
C_i^*, C_o^*	dimensionless concentrations at inner and outer radii respectively
D	mass diffusivity ..... $m^2\,s^{-1}$
e_r	unit vector in r-direction
e_φ	unit vector in φ-direction
g	acceleration of gravity ..... $m\,s^{-2}$
Gr_S	solutal Grashof number based on the gab width, $Gr_S = g\beta_S(c_i - c_o)b^3/\nu^2$
Gr_T	thermal Grashof number based on the gab width, $Gr_T = g\beta_T(T_i - T_o)b^3/\nu^2$
h	heat transfer coefficient ..... $W\,m^{-2}\,K^{-1}$
h_s	solutal transfer coefficient ..... $m\,s^{-1}$
K	fluid thermal conductivity ..... $W\,m^{-1}\,K^{-1}$
Le	Lewis number, $Le = \alpha/D = Sc/Pr$
N	buoyancy ratio, $N = \beta_S\Delta C/\beta_T\Delta T$, or $N = Ra_S/Ra_T$
Nu	average Nusselt number, $Nu = \frac{hb}{K}$
Nu_φ	local Nusselt number, $Nu_\varphi = -(R\frac{\partial\theta/\partial R}{Nu_{\text{cond}}})_{R=R_i}$
P	pressure ..... $N\,m^{-2}$
P^*	dimensionless pressure
Pr	Prandtl number, $Pr = \nu/\alpha$
r	radial coordinate
r_i, r_o	inner and outer radii respectively ..... m
R	dimensionless radial coordinates, $R = r/b$
R_i, R_o	dimensionless inner and outer radii respectively
Ra_S	solutal Rayleigh number based on the gab width, $Ra_S = Gr_S^*Pr = g\beta_S(c_i - c_o)b^3/\alpha\nu$
Ra_T	thermal Rayleigh number based on the gab width, $Ra_T = Gr_T^*Pr = g\beta_T(T_i - T_o)b^3/\alpha\nu$
Re	rotational Reynolds number, $Re = \omega r_i b/\nu$
Sc	Schmidt number, $Sc = \nu/D$
Sh	average Sherwood number, $Sh = \frac{h_S b}{D}$
Sh_φ	local Sherwood number, $Sh_\varphi = \ln(\frac{R_i}{R_o})(R\frac{\partial C^*}{\partial R})_{R=R_i}$
T	local temperature ..... K
T_i, T_o	temperatures at inner and outer radii respectively ..... K
ΔT	temperature difference, $(T_i - T_o)$ ..... K
u	velocity vector ..... $m\,s^{-1}$
U	dimensionless velocity vector, $U = u/\omega r_i$

Greek symbols

β_T	Coefficient of thermal expansion ..... K^{-1}
β_S	Coefficient of solutal expansion ..... kg^{-1}
α	Thermal diffusivity ..... $m^2\,s^{-1}$
φ	angular coordinate
ω	angular velocity ..... $rad\,s^{-1}$
Ψ	dimensionless stream function
θ	dimensionless temperature, $(T - T_o)/(T_i - T_o)$
ν	Kinematic viscosity ..... $m^2\,s^{-1}$
ρ	Fluid density ..... $kg\,m^{-3}$

structure. Later on, the same authors [6] studied the effect of thermal Rayleigh number and Lewis number on double-diffusive natural convection in a closed annulus. The results illustrated that the thermal Rayleigh number and the Lewis number were found to influence the buoyancy ratios at which flow transition and flow reversal occurred. In addition, several studies were reported on double-diffusive natural convection in a vertical annulus. Teamah and Shoukri [7] studied the effect of radius ratio, aspect ratio and buoyancy ratio on the double diffusive natural convection in vertical annulus enclosures. Their results cover a radius ratio from 1 to 5, aspect ratio from 1 to 4 and buoyancy ratio from 10^{-3} to 10^3.

Mixed heat transfer in a horizontal rotating annulus with thermal driven flows only, was early studied numerically by Fusegi et al. [8] and Lee [9]. Recently, Yoo [10–14] conducted a series of numerical studies for a horizontal rotating annulus. These studies cover a wide range of Grashof and Prandtl numbers. Also, Teamah et al. [15] studied the same geometry used by Yoo with different parametric study for rotational Reynolds number, radius ratio and Prandtl number. They studied the transitions in flow from no cells to one cell and from one cell to two cells.

For cross double diffusive convection Shi and Lu [16,17] studied the double diffusive natural convection in a vertical cylinder with radial temperature and axial solutal gradients. Their study was focused on the effect of the buoyancy ratio on the evolution of the flow field, temperature and solute field in the cavity. In their study the following parameters were fixed at Prandtl number, $Pr = 7$, the Lewis number, $Le = 5$, the thermal Grashof number, $Gr_T = 10^7$, and the aspect ratio of the enclosure, $A = 2$.

Sung et al. [18] reported on a rotating horizontal annulus, where the external temperature gradient is imposed horizontally while the solutal gradient is applied in the vertical direction. They conducted a parametric study to present the qualitative features of flow patterns and isotherms. Lee et al. [19,20] have investigated the effect of rotation in a double-diffusive convection for a stably stratified fluid within an annulus. They showed the effect of rotation on the development and merging of the multi-layered flow structure and various field variables. Al-Amiri and Khanafer [21] investigated the laminar flow and heat transfer characteristics of a binary fluid within a two-dimensional horizontal annulus with cooled rotating outer cylinder. They assumed the inner cylinder to be the heated wall and the source for the species concentration. They conducted a parametric study to present the qualitative features of flow patterns, isotherms and isoconcentration. Their studied parameters are Reynolds number, Lewis number, Buoyancy ratio number, Rayleigh number, Prandtl number, and the annulus gap width ratio.

From the previous review, the double diffusive mixed convection between rotating cylinders is very important in many engineering applications, and it has a shortage in publications and design correlations. Therefore, the present investigation is devoted to study this configuration. The inner cylinder is isothermally heated and capable of rotating at a constant angular velocity. Also the inner cylinder is considered to be a source for the concentration. On the other hand, the outer cylinder is considered fixed, isothermally cold and a sink for the concentration. The annulus radius ratio is assumed fixed at 0.5. The study covers ranges for thermal Rayleigh number from 10^2 to 10^6. The small value for Rayleigh number represents the conduction regime. While the high Rayleigh number is close to transition value to turbulent regime. Also, this study covers a range for buoyancy ratio from -20 to 20. This range covers both aiding and opposing flow regimes. In addition, the study covers a range for Lewis number from 0.1 to 10, this value is within the values taken by many authors in this field.

2. Mathematical model

Two long concentric horizontal cylinders with gab width, b, are considered. The geometry of the problem is shown in Fig. 1. Both of the two cylinders are held at constant but different temperatures and concentrations of T_i, C_i and T_o, C_o ($T_i > T_o$) and ($C_i > C_o$). The temperature gradient generates the natural thermal diffusive force and the concentration gradient generates the natural solutal diffusive force. The inner cylinder is considered able to rotate anti-clock wise at a constant angular velocity to create the forced convection. In addition, the flow in the annular region is assumed to be Newtonian, two-dimensional, steady and laminar. Also, all thermo-physical properties of the fluid are taken to be constant except for the density variation in the buoyancy term, where the Boussinesq approximation is considered to be linearly proportional to both temperature and concentration such that:

$$\rho = \rho_o\big[1 - \beta_T(T - T_o) - \beta_s(C - C_o)\big] \tag{1}$$

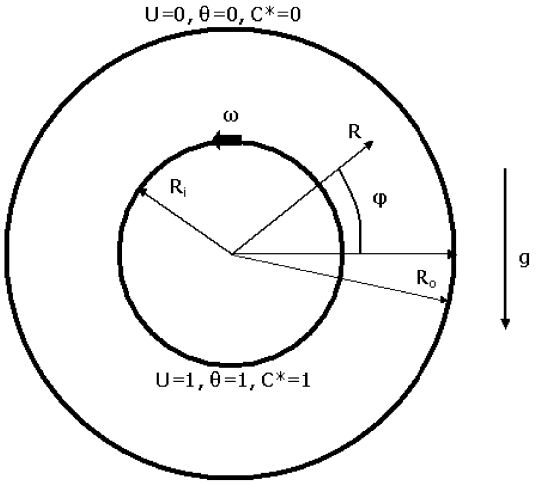

Fig. 1. A schematic of the problem.

To cast the governing equations in the dimensionless form, the following dimensionless variables are introduced to the governing equations:

$$R = \frac{r}{b}, \qquad U = \frac{u}{\varpi r_i}, \qquad \theta = \frac{T - T_o}{T_i - T_o}$$
$$C^* = \frac{C - C_o}{C_i - C_o}, \qquad P^* = \frac{P}{\rho(\varpi^2 r_i)} \tag{2}$$

The dimensionless form of governing equations for the continuity, momentum, thermal energy and species transport in the cylindrical coordinate are as follows:

$$\nabla U = 0 \tag{3}$$

$$(U.\nabla)U = -\nabla P^* + \frac{1}{Re}\nabla^2 U + \frac{Gr_T}{Re^2}\big[(\theta + NC^*)\sin(\phi)e_r + (\theta + NC^*)\cos(\phi)e_\phi\big] \tag{4}$$

$$(U.\nabla)\theta = \frac{1}{Pr\,Re}\nabla^2\theta \tag{5}$$

$$(U.\nabla)C^* = \frac{1}{Sc\,Re}\nabla^2 C^* \tag{6}$$

Where U is the dimensionless velocity vector, P^* is the dimensionless acting pressure. $Re = \omega r_i b/\nu$, is the rotational Reynolds number, $N = Gr_s/Gr_T$ is the buoyancy ratio, $Sc = \nu/D$ is the Schmidt number, $Pr = \nu/\alpha$ is the Prandtl number.

The dimensionless boundary conditions are:

$$U = 1.0, \quad V = 0, \quad \theta = 1.0 \quad \text{and}$$
$$C^* = 1.0, \quad \text{at } R = R_i \tag{7a}$$

$$U = 0, \quad V = 0, \quad \theta = 0 \quad \text{and} \quad C^* = 0, \quad \text{at } R = R_o \tag{7b}$$

By defining the Nusselt number as the ratio between the actual heat transfer rate and the heat transferred by pure conduction, then the local Nusselt number along the inner cylinder is calculated as

$$Nu_\varphi = -\left(R\frac{\partial\theta/\partial R}{Nu_{\text{cond}}}\right)_{R=R_i} \tag{8}$$

Where Nu_{cond} is the Nusselt number in the case of heat transfer through the annulus by pure conduction and given by

$$Nu_{\text{cond}} = \frac{1}{\ln\frac{R_o}{R_i}} \tag{9}$$

From Eqs. (8) and (9), the final form of the local Nusselt number is as follows:

$$Nu_\varphi = \ln\left(\frac{R_i}{R_o}\right)\left(R\frac{\partial\theta}{\partial R}\right)_{R=R_i} \tag{10}$$

The average Nusselt number is calculated from integrating the local value over the circumference of the inner cylinder as follows:

$$Nu = \frac{1}{2\pi}\int_0^{2\pi} Nu_\varphi\, d\varphi \tag{11}$$

Similarly, we can calculate both local and average Sherwood numbers as follows:

$$Sh_\varphi = \ln\left(\frac{R_i}{R_o}\right)\left(R\frac{\partial C^*}{\partial R}\right)_{R=R_i} \tag{12}$$

and

$$Sh = \frac{1}{2\pi}\int_0^{2\pi} Sh_\varphi \, d\varphi \tag{13}$$

The dimensionless stream function Ψ, is calculated by integrating the dimensionless velocity in the angular direction as follows:

$$\Psi = \int_{R_i}^{R} (-V)\, dR \tag{14}$$

3. Solution procedure

The governing equations were solved by using the finite volume technique developed by Patankar [22]. This technique was based on the discretization of the governing equations using the central differencing in space. The number of grids was checked. The deviations between the results obtained for domain (52×42) and (202×162) were less than 0.2%. Therefore, through the study, the domain size was (90×72). To calculate both Nusselt and Sherwood numbers, we use numerical differentiations, $(\partial\theta/\partial R)_{R=R_i}$ and $(\partial\theta/\partial R) = \mathrm{Lim}_{\Delta R\to 0}(\Delta\theta/\Delta R)$. Therefore, at the cylinder wall we need very fine grids to obtain accurate results. In R direction, the height of 5 control volumes close to both inner and outer boundaries were 1/4 the heights of the central control volumes. In ϕ direction, we do not need numerical differentiations. Therefore, a uniform grid was taken in this direction. The discretization equations were solved by the Gauss–Seidel method. The iteration method used in this program is a line-by-line procedure, which is a combination of the direct method and the resulting Tri Diagonal Matrix Algorithm (TDMA). The accuracy was defined by the change in the average Nusselt number and the other dependent variables through one hundred iterations to be less than 0.01% from its value. The check showed that 3000 iterations were enough for all of the investigated values.

4. Program validation and comparison with previous work

The subject of this investigation is a new and an important field of research. Therefore, a computer program was constructed in a general form to solve most parameters affecting the double diffusive mixed convection in rotating annulus. Such as either cylinder that can rotate or rotating the two cylinders in both the same and opposite directions. Firstly, the program was run when the outer cylinder was rotating. The dimensionless temperature and concentration at the inner cylinder were kept constant and their values equal one, while their values at the outer cylinder equal to zero. This condition was the same as that studied by Amiri and Khanafer [21]. Fig. 2 plots both the average Nusselt and Sherwood numbers over a range of buoyancy ratio from −10 to 10. Through the figure the value of Lewis number was kept constant at one, the thermal Rayleigh number at 10^4, Prandtl number at 0.7 and rotational Reynolds number as 100. The figure shows a comparison between the results obtained from the program used in this investigation and

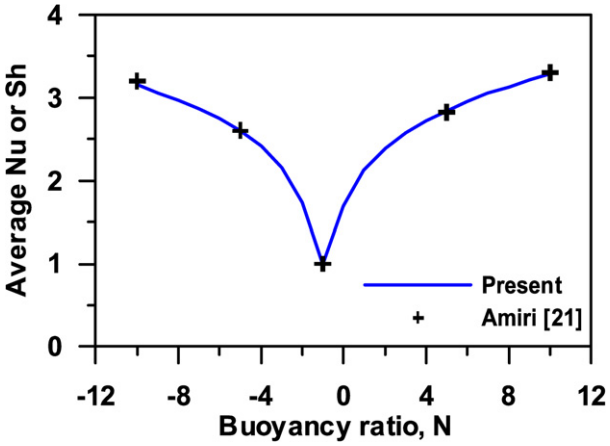

Fig. 2. Comparison with Amiri [21], Outer cylinder rotates, $Le = 1$, $Re = 100$ and $Ra_T = 10^4$.

the results published by Amiri [21]. The maximum deviation between the results was within two percent. Fig. 3 plots the effect of Lewis number on both the average Nusselt and Sherwood numbers when the outer cylinder was rotating and the rotational Reynolds number was 100. The graph compared the predicted results from the designed program to that given by Amiri [21] for a range of Lewis number from zero to ten. The figure shows a good agreement for the values of Nusselt number, the maximum deviation was within one percent. On the other hand, the values for the average Sherwood number calculated by the computer program are slightly lower than that of Amiri [21]. The results are very close at low Lewis number, but the maximum deviation at higher values of Lewis number was less than five percent.

5. Results and discussions

Different runs were carried out to explain the effects of thermal Rayleigh, Lewis numbers and buoyancy ratio on the studied problem. The results were divided into local results and average results. The streamlines, temperature and concentration patterns as well as the local Nusselt and Sherwood numbers were examined as local results. These local results explore the phenomena that appeared in the average value. While the average results contained the average values for both Nusselt and Sherwood numbers, which are used in heat and mass transfer calculations as well as the design of thermal equipment. All results were performed with $Pr = 0.7$, $Re = 100$ and radius ratio $= 0.5$.

The effect of Rayleigh number on streamlines and isotherms is shown in Fig. 4. In order to highlight the effect of Ra alone, both Lewis number and buoyancy ratio were kept constant at values equal one. When Lewis number equals one, the thermal diffusivity equals to the mass diffusivity. This means that the isothermal lines are congruent with the isoconcentration lines. Therefore, the isotherms were only presented. The Rayleigh number was varied over a range from 10^2 to 10^6. The lower limit represents the forced convection regime, while the upper limit represents the natural convection regime. For upper limits the flow is mainly induced by the buoyancy force, which was generated due to the temperature and concentration gradients.

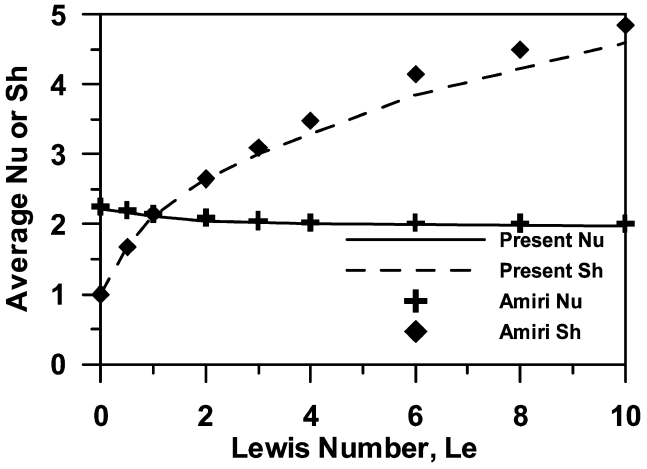

(a)

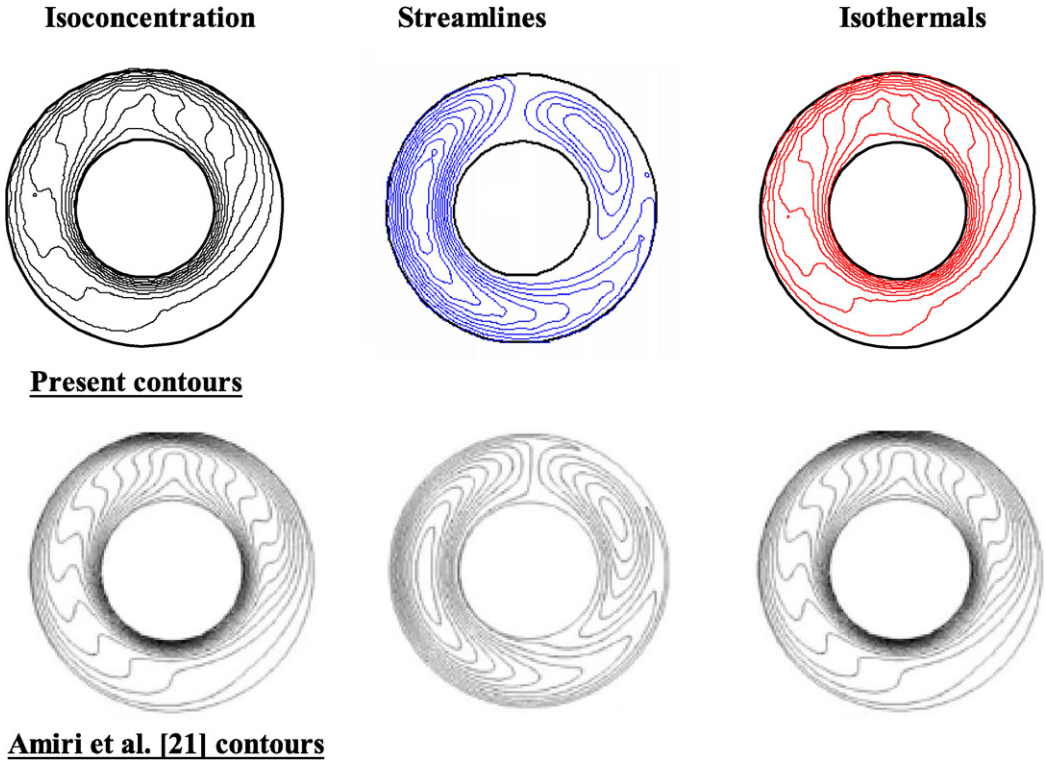

(b)

Fig. 3. Comparison with Amiri et al. [21], Outer cylinder rotates, $N = 1$, $Re = 100$ and $Ra_T = 10^4$. (a) Average Sherwood number; (b) Isoconcentration, streamlines and isothermals.

On the other hand, the effect of forced flow disappeared. The streamlines consist of one pair of cells, one on the right and the other on the left portion of the cavity. The two cells are similar in shape and symmetric about a vertical line passing through the cavity center. Also, the isotherms are symmetric about this line and very close at the bottom of the inner cylinder. This means a high rate for heat and mass transfer due to natural convection. When the value of Rayleigh number is changed to 10^5, the effect of rotation appears. Due to the rotation of inner cylinder in anti-clock wise direction, in the right portion of the cavity the forced convection flow is added to the natural convection flow. Conversely, they oppose each other in the left portion. Therefore, the right cell seems stronger than the left one. In addition, the rotation pushes the cells in the anti-clock wise direction. As the Rayleigh number is decreased, the effect of rotation appears strongly. The rotation drags the right cell, and the left cell becomes weaker. An isothermal plume is appeared at the top of the inner cylinder, the rotation moves this plume towards the left direction. At low Rayleigh number, $Ra = 10^2$ both the left weak cell and isothermal plume are disappeared. In this situation, the forced convection is dominated and the streamlines and isotherms become concentric rings around the inner cylinder. This distribution for streamlines is similar to the Couette flow patterns. The flow strength is very high close to the inner cylinder. Conversely, it is very weak nearer to the outer cylinder.

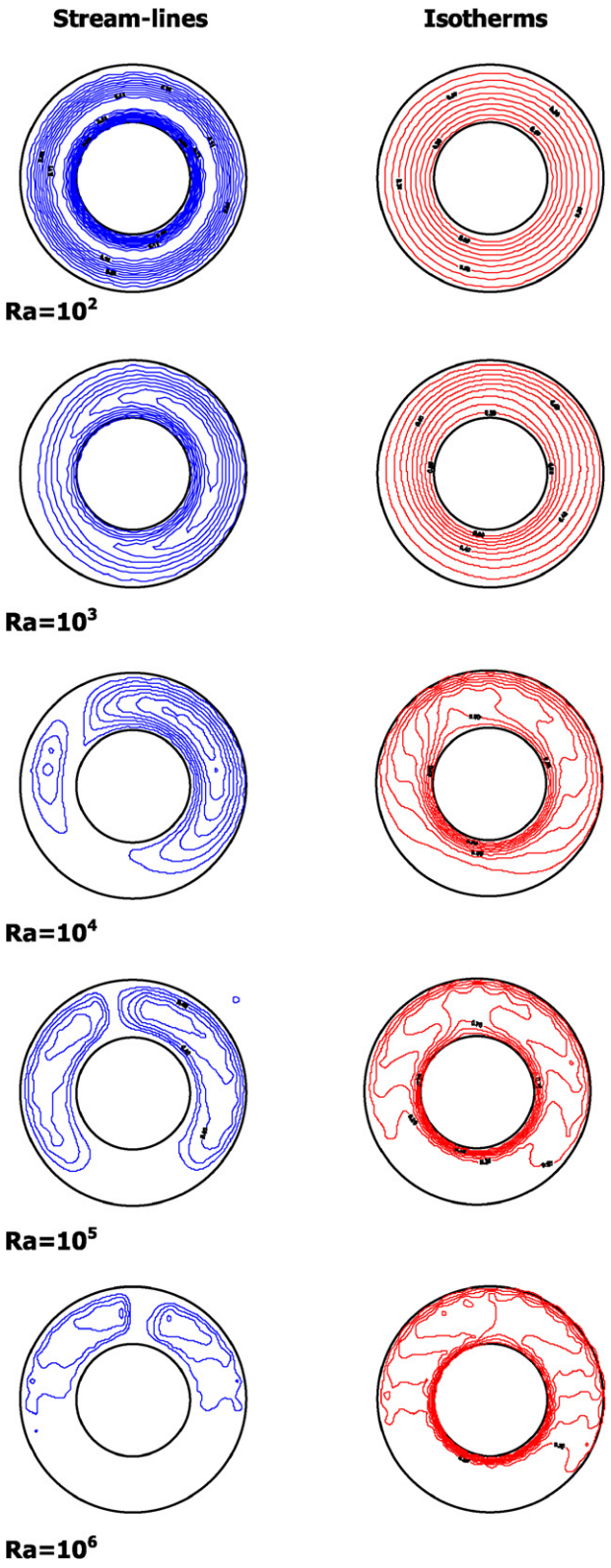

Fig. 4. Effect of *Ra* on stream lines and isotherms. $Le = 1.0$ and $N = 1.0$.

The effect of thermal Rayleigh number on both local Nusselt and Sherwood numbers over the inner cylinder is shown in Fig. 5. At low Rayleigh number, the forced convection dominated and the isotherms are concentric circles as mentioned above. The variation of the local values along angle φ, are very

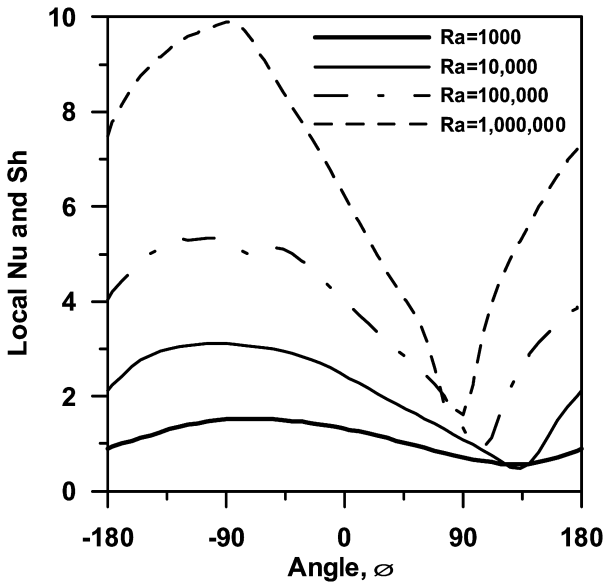

Fig. 5. Effect of thermal Rayleigh number on local Nusselt and Sherwood numbers, $Le = 1$ and $N = 1$.

small and the local *Nu* seems constant. This variation is increased with Rayleigh number. At the thermal plume position, the direction of the cells depart away from the inner cylinder. Therefore, the local Nusselt number has a minimum value at this position. On the other hand, at the bottom of the inner cylinder the local Nusselt has a maximum value. Also, as expected the local Nusselt and Sherwood numbers increased with Rayleigh number.

The effects of Lewis number on the streamlines, isotherms and isoconcentration lines are plotted in Fig. 6. To study the effect of Lewis number, the Rayleigh number was kept constant at 10^4, at this value of *Ra* the Richardson number, $Ri = Ra_T/Re^2 = 1$. This makes the order of magnitude for forced and natural flows equal. Therefore, the fluid is driven by mixed convection. In addition the value of buoyancy ratio was kept constant and equals to unity. The Lewis number was varied over a range from 0.1 to 10. At Lewis number equals 0.1, the mass diffusivity is higher than the thermal diffusivity and the mass diffusion rate is stratified in the radial direction. The rotational effect moves the thermal plume as well as the two cells in the direction of rotation. As the Lewis is increased to one, the right cell (aiding flow region) becomes stronger and both isotherms and concentration lines are typical. At Lewis number $Le = 5$, the mass plume becomes stronger and diffuses through the domain. The thickness of solutal boundary layer is thinner than the thermal boundary layer around the inner cylinder. This means that the thermal resistance is higher than the solutal resistance. Therefore, the mass transfer rate is higher than the heat transfer rate. The strength of streamlines is decreased with Lewis number. On the other hand, the Lewis number has invisible significant effect on the isotherms.

The dependence of both local Nusselt and Sherwood numbers over the circumference of the inner cylinder on the Lewis number is displayed in Figs. 7 and 8. In general, the local Sherwood number increases with Lewis number. On the other hand,

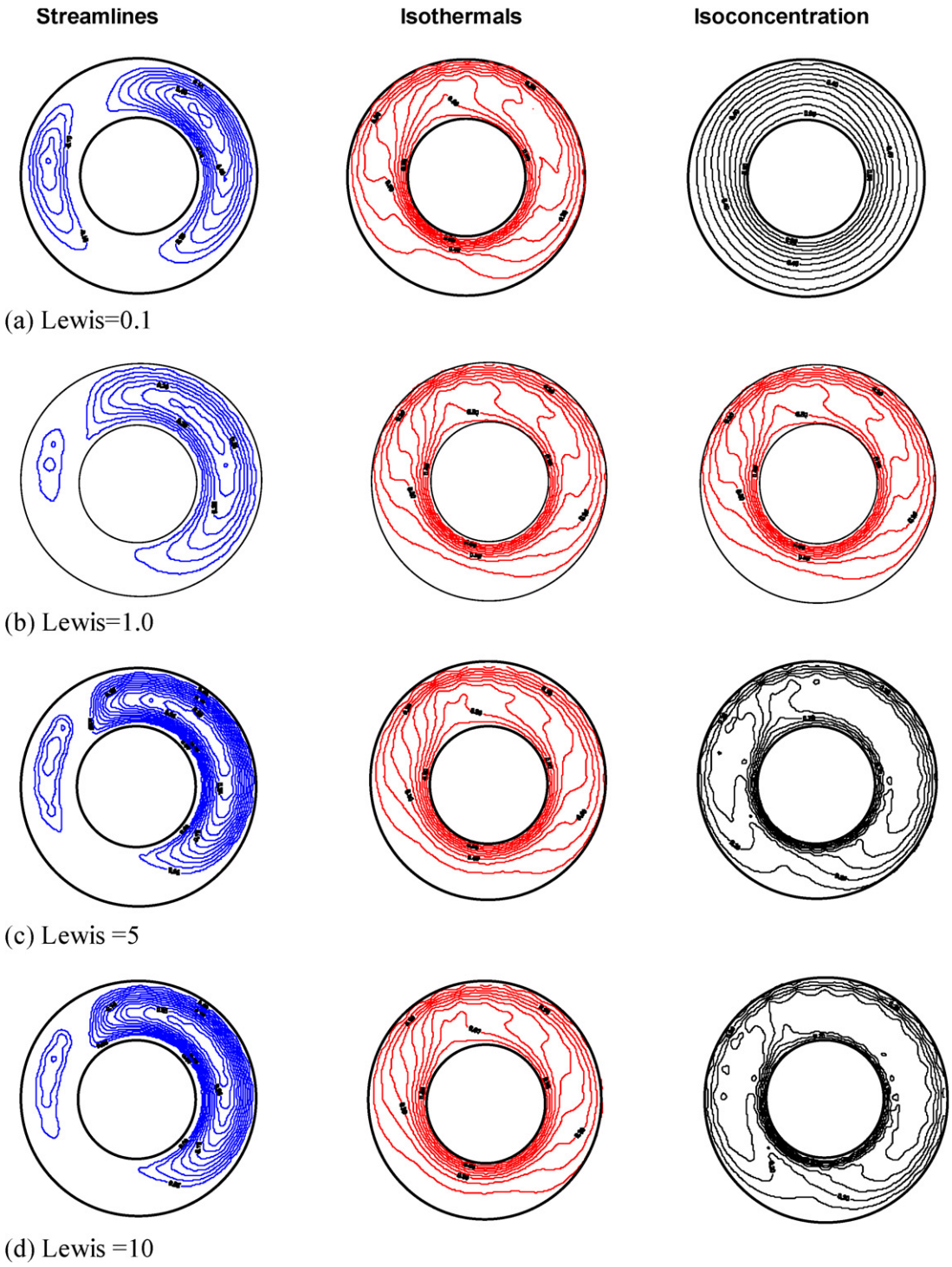

Fig. 6. Effect of Lewis number on streamlines, isotherms and isoconcentration $Ra = 10^4$ and $N = 1$.

the local Nusselt slightly dips as the Lewis number is increased. The predicted local *Nu* and *Sh* have minimum values at the thermal plume angle. Furthermore, they have maximum values in opposite to the position of minimum values. At this angle, the circulating cells are incoming to the inner cylinder.

The dependence of streamlines and isotherms on the buoyancy ratio is shown in Fig. 9. To explore the effect of buoyancy ratio, the thermal Rayleigh number is kept constant at 10^4 and the value of Lewis number equals to unity. To explore the effect of both negative and positive values of buoyancy ratio, N is selected to be varied from -20 to 20. Negative values of N, indicate that the volumetric expansion coefficient with mass fraction holds a negative value for the prescribed temperature range. At $N = -20$ (dominated mass transfer regime), the flow consists of 2 cells one cell on the right and the other one on the left portion. On the left portion, the natural flow is aiding to the forced flow. Therefore, the left cell is stronger than the right. Furthermore, the rotational speed drags the left cell down-

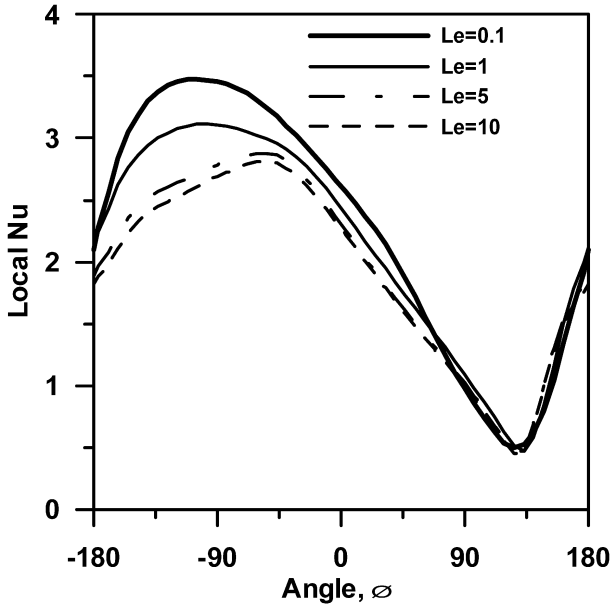

Fig. 7. Effect of Lewis number on local Nusselt number, $Ra_T = 10^4$ and $N = 1$.

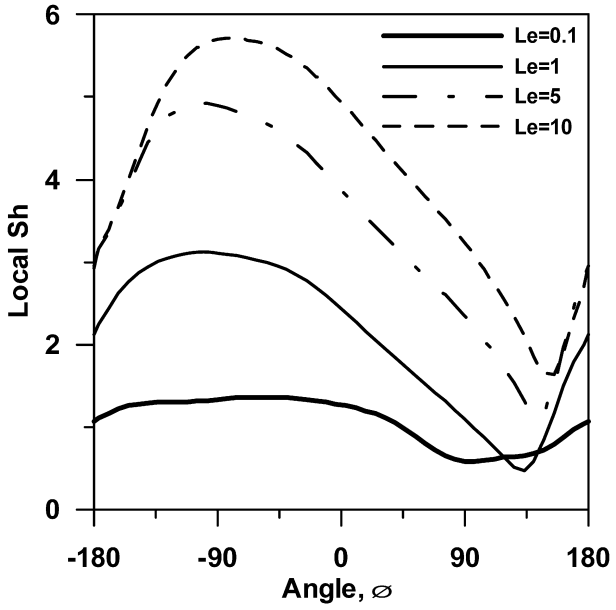

Fig. 8. Effect of Lewis number on local Sherwood number, $Ra_T = 10^4$ and $N = 1$.

ward and the right one upward. In addition, a thermal plume is noticed below the inner cylinder and tilted in the rotational direction. In the region over the inner cylinder, the isotherms are stratified. As the buoyancy ratio is increased the effect of forced flow is pronounced. This is observed by continuing growth for the adding flow cell and diminishes for the opposing flow cell relatively. Furthermore, the tilting of the thermal plumes in the rotation direction is increased. As N is increased to -1, the weaker cell disappeared and both the streamlines and isotherms are concentric circles around the inner cylinder and the flow looks like the Couette flow pattern as mentioned before. Apparently, as the buoyancy ratio equals to zero, the pure mixed heat transfer convection is dominated. The weaker cell is renewed but on the left portion. This was observed by Yoo [14] and Teamah et al. [15]. Employing a positive values of the buoyancy ratio causes a reversal in the basic flow pattern and isotherms. They are showing reverse behaviors along the horizontal centerline of the annulus as compared to the negative values for the buoyancy ratio.

The prediction of the effect of buoyancy ratio on both local Nusselt and Sherwood numbers is presented in Fig. 10 for negative values of N and in Fig. 11 for positive values of N. As is known, for $N = 1$, the values of both local Nu and Sh are fixed and equal to unity. This means that the conduction mode is dominated for both heat and mass transfer. As the buoyancy ratio depart from unity, the mixed convection pronounces and local values increase. Also, it is seen that the local values for negative and positive buoyancy ratios have reversed shape along the horizontal centerline of the annulus. In addition, for low absolute values of N, the positions of maximums and minimums are shifted from the top and bottom of inner cylinder in the direction of rotation. Furthermore, as the absolute value of buoyancy ratio is increased the natural convection is dominated and the shift is decreased.

The combined effect of both Lewis number and buoyancy ratio on the average value of Nusselt number is illustrated in Fig. 12. In the figure, the thermal Rayleigh number is kept constant at 10^4. At constant buoyancy ratio, the average Nusselt number decreases as the Lewis is increased. At buoyancy ratio over a range from $N = -1$ to $N = 2$, the average Nusselt number attains a slight dip and then assumes an asymptotic value with the increase in Lewis number. In general the average Nusselt number increases with the increase in the absolute value of buoyancy ratio. The predicted values of average Nusselt number over the range of the investigated buoyancy ratio and Lewis number are correlated in the following form:

For $N > 0$

$$Nu_{\mathrm{av}} = 2.102 Le^{-0.098} N^{0.137} \tag{15}$$

and for $N < -1$

$$Nu_{\mathrm{av}} = 1.303 Le^{-0.162} |N|^{0.295} \tag{16}$$

The validity ranges for these correlations are; $0.1 \leqslant Le \leqslant 10$ and $-20 \leqslant N \leqslant 20$ with standard deviations 0.038 and error within 5%. A comparison for these correlations and numerical results was presented in Fig. 13

The combined effect of both Lewis number and buoyancy ratio on the average value of Sherwood number is shown in Fig. 14. Also the thermal Rayleigh number has a constant value of 10^4. For a constant buoyancy ratio, the average Sherwood number increases with Lewis number. At $Le = 0.1$, the mass diffusivity is high compared with the thermal diffusivity, therefore the absolute value for buoyancy ratio has a minor effect on the predicted values of Sherwood number. In addition, at buoyancy ratio, $N = -1$, the conduction regime is dominated and the Nusselt and Sherwood numbers have a minimum value. This value equals one. Also, both average Nusselt and Sherwood numbers variations are symmetrical about a vertical line with $N = -1$. Furthermore, the rate of increase is high near the symmetrical line. The predicted values of average Sherwood

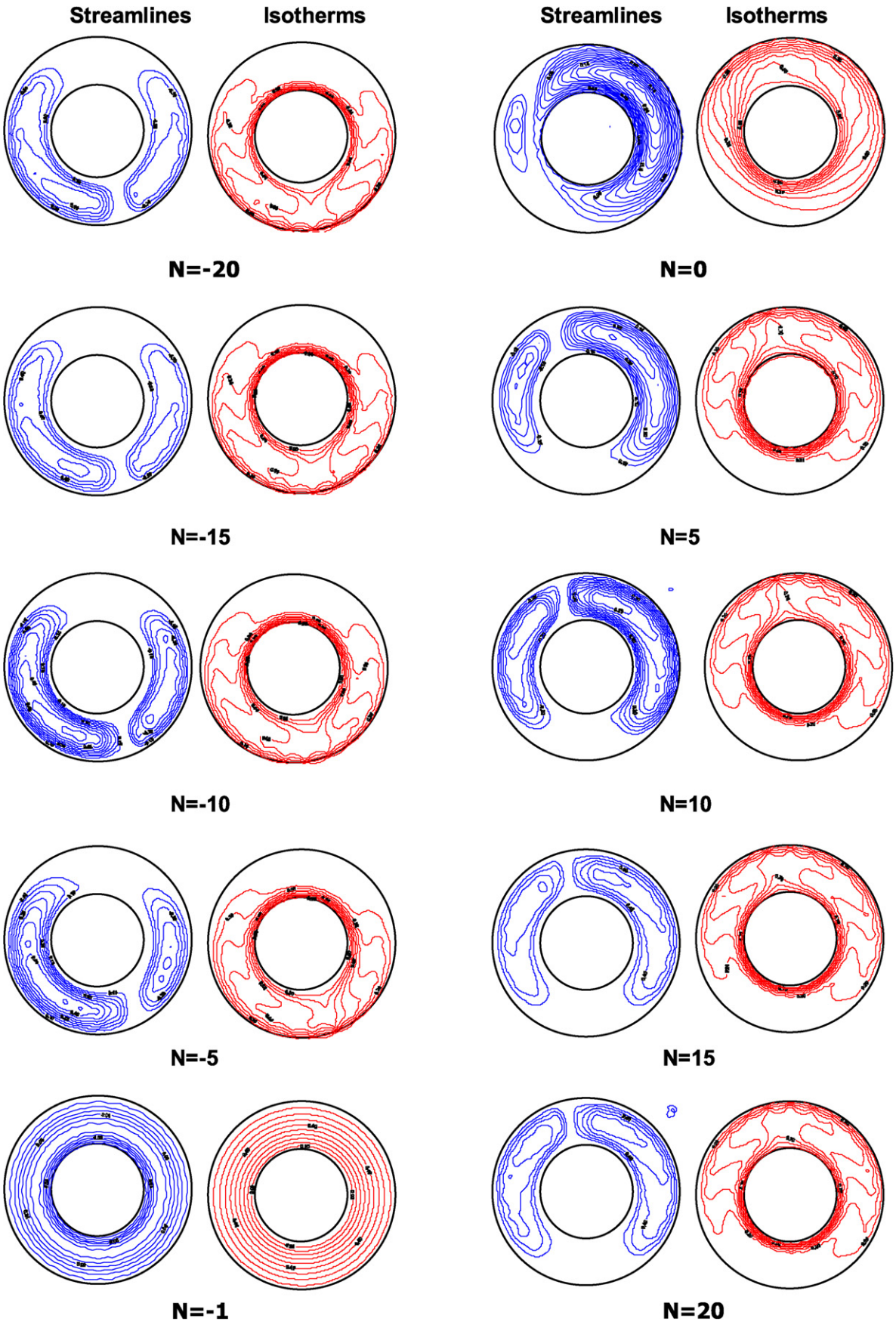

Fig. 9. Effect of buoyancy ratio on streamlines and isotherms $Ra_T = 10^4$ and $Le = 1$.

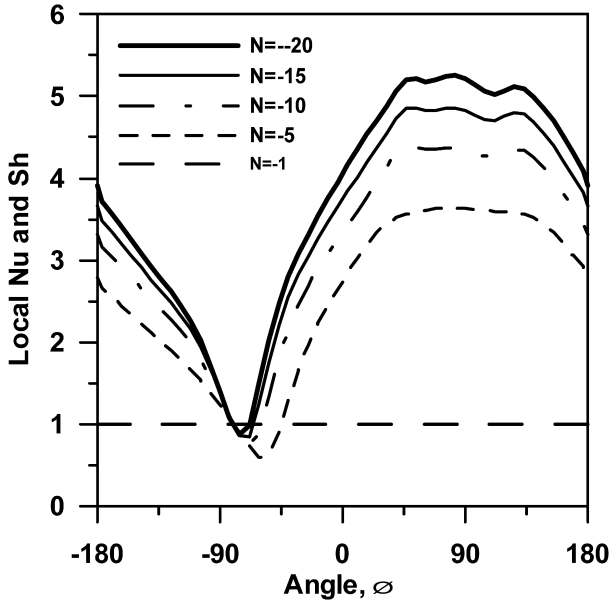

Fig. 10. Effect of N on both local Nu and Sh, $N < 0$, $Le = 1$ and $Ra_T = 10^4$.

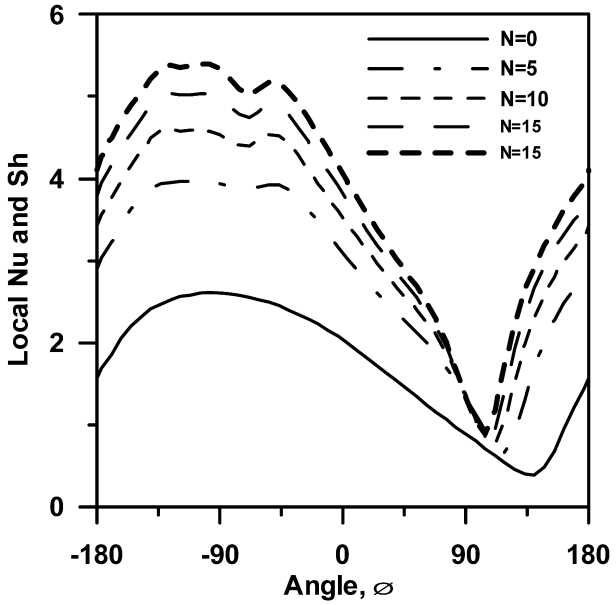

Fig. 11. Effect of N on both local Nu and Sh, $N > 0$, $Le = 1$ and $Ra_T = 10^4$.

number over the range of the investigated buoyancy ratio and Lewis number are correlated in the following form:

For $N > 0$

$$Sh_{av} = 2.041 Le^{0.297} N^{0.181} \tag{17}$$

and for $N < -1$

$$Sh_{av} = 1.067 Le^{0.247} |N|^{0.44} \tag{18}$$

The validity ranges for these correlations are $0.1 \leqslant Le \leqslant 10$ and $-20 \leqslant N \leqslant 20$ with standard deviations 0.038 and error within 4.8%.

The dependence of average Nusselt and Sherwood numbers on the thermal Rayleigh number is presented in Fig. 15. To highlight the effect of Rayleigh number, the Lewis number is

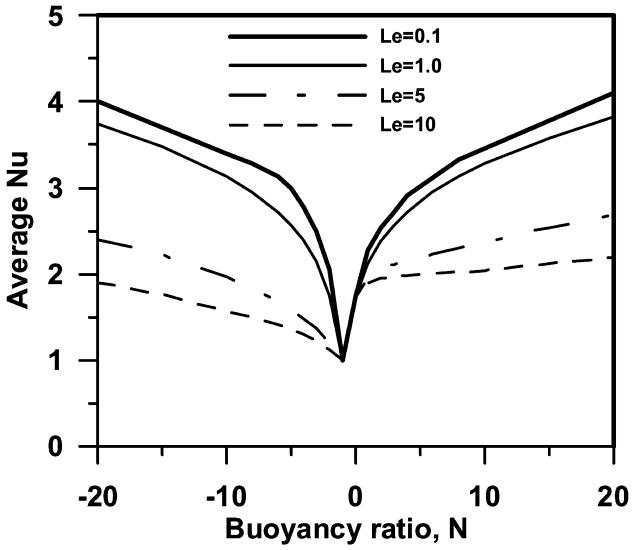

Fig. 12. Effect of Lewis number on average Nusselt number, $Ra_T = 10^4$ and $Re = 100$.

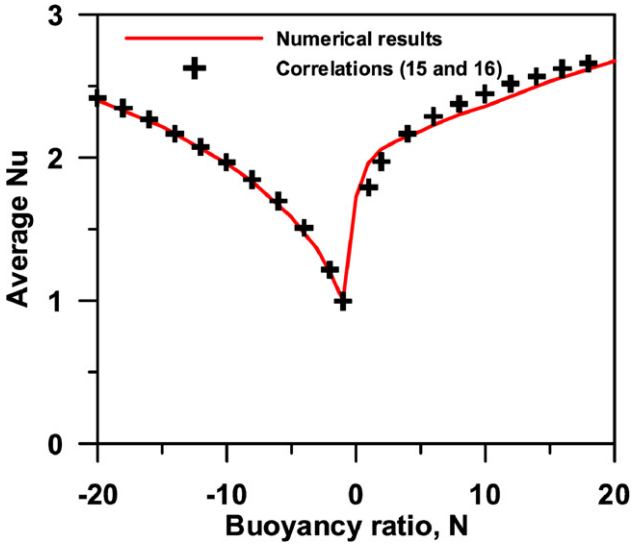

Fig. 13. Comparison between the numerical results and correlations (15 and 16), $Le = 5$.

kept constant and equals to unity. It can be seen that, the values of both Nusselt and Sherwood numbers increase if either thermal Rayleigh number or absolute value of buoyancy ratio are increased. For small thermal Rayleigh number, the forced flow is dominated and the buoyancy ratio has a small effect on the predicted Nusselt and Sherwood numbers. Moreover, it can be noticed that, at buoyancy ratio equals negative one the predicted Nusselt and Sherwood numbers equal one for all values of thermal Rayleigh number. In this case, the convective flows oppose each other and the conduction regime is dominated. Also, there is a symmetry about the vertical line with buoyancy ratio equals negative one. The predicted values for average Nusselt and Sherwood are correlated in the following form:

For $N > 0$

$$Nu_{av} = 0.185 Ra_T^{0.257} N^{0.21} \tag{19}$$

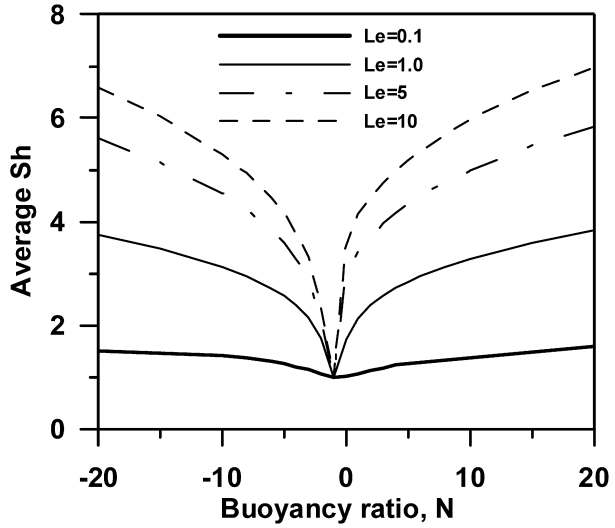

Fig. 14. Effect of Lewis number on average Sherwood number, $Ra_T = 10^4$ and $Re = 100$.

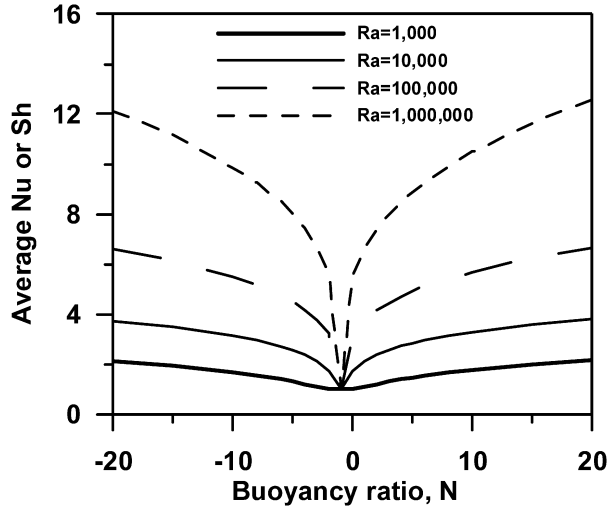

Fig. 15. Effect of thermal Rayleigh number Ra_T on average Nu and Sh numbers $Le = 1$ and $Re = 100$.

and for $N < -1$

$$Nu_{\text{av}} = 0.137 Ra_T^{0.256} |N|^{0.32} \tag{20}$$

The validity ranges for these correlations are $10^3 \leqslant Ra_T \leqslant 10^6$ and $-20 \leqslant N \leqslant 20$ with standard deviations 0.038 and error within 2.8%.

6. Conclusions

This investigation is concerned with the numerical simulation of double diffusive flow in a two-dimensional horizontal annulus with the inner cylinder rotating at constant speed. The thermal and solutal gradients were maintained by subjecting the inner cylinder to higher values than the outer one. The following remarks were concluded.

(1) At buoyancy ratio equals negative one, the conduction regime is dominated and the streamlines, isotherms as well as the isoconcentration lines are concentric circles. Furthermore, the average values for both Nusselt and Sherwood numbers equal one for all cases studied in this research.

(2) In a small absolute value of buoyancy ratio, the Lewis number has a very minor effect on the average Nusselt number. The Nusselt number slightly decreases if the Lewis number is increased. On the other hand, the effect of Lewis number is obvious for a higher values for the absolute buoyancy ratio. Conversely, the average Sherwood number increases by increasing the Lewis number.

(3) At lower value of thermal Rayleigh number, the forced convection is dominated. As the thermal Rayleigh number is increased, thermal and concentration plumes appeared. These plumes are tilted towards the direction of rotation. At high thermal Rayleigh number, the natural convection is dominated. At $Ra_T = 10^6$ the streamlines show that the flow consists of 2 cells. The two cells are symmetric about the vertical centerline of the cavity.

(4) In all conditions, the average Nusselt and Sherwood numbers increase if either the thermal Rayleigh number or the absolute value of buoyancy ratio is increased.

(5) Usefully correlations for both average Nusselt and Sherwood numbers in terms of Lewis number and buoyancy ratio are given by:
For $N > 0$

$$Nu_{\text{av}} = 2.102 Le^{-0.098} N^{0.137}$$

and for $N < -1$

$$Nu_{\text{av}} = 1.303 Le^{-0.162} |N|^{0.295}$$

For $N > 0$

$$Sh_{\text{av}} = 2.041 Le^{0.297} N^{0.181}$$

and for $N < -1$

$$Sh_{\text{av}} = 1.067 Le^{0.247} |N|^{0.44}$$

(6) Lastly, for $Le = 1$, the average Nusselt and Sherwood numbers are correlated in terms of thermal Rayleigh number and buoyancy ratio in the following forms:
For $N > 0$

$$Nu_{\text{av}} = 0.185 Ra_T^{0.257} N^{0.21}$$

and for $N < -1$

$$Nu_{\text{av}} = 0.137 Ra_T^{0.256} |N|^{0.32}$$

The accuracy of the above correlation is given in text and these correlations can be used in heat and mass transfer problems as well as the design of thermal equipment.

References

[1] C.Y. Hu, M.M. EL-Wakil, Simultaneous heat and mass transfer in a rectangular cavity, in: Proc. 5th Int. Heat Transfer Conf., vol. 5, 1974, pp. 24–28.
[2] S. Ostrach, Natural convection with combined driving forces, Physico Chem. Hydrdyn. 1 (1980) 233–247.
[3] S. Ostrach, Natural convection heat transfer in cavities and cells, in: 7th Int. Heat Transfer Conf., Munich, 1982, vol. 1, pp. 365–379.

[4] S. Ostrach, Fluid mechanics in crystal growth—the 1982 Freeman scholar lecture, J. Fluid Eng. 105 (1983) 5–20.
[5] P.W. Ship, M. Shoukri, M.B. Carver, Double-diffusive natural convection in a closed annulus, Numer. Heat Transfer: Part A 24 (1993) 339–356.
[6] P.W. Ship, M. Shoukri, M.B. Carver, Effect of thermal Rayleigh and Lewis numbers on double-diffusive natural convection in a closed annulus, Numer. Heat Transfer: Part A 24 (1993) 451–465.
[7] M.A. Teamah, M. Shoukri, The effect of aspect and curvature ratios on double-diffusive natural convection in a vertical annulus, Alexandria J. 34 (2) (1995) 95–105.
[8] T. Fusegi, B. Farouk, K.S. Ball, Mixed-convection flows within a horizontal concentric annulus with a heated rotating inner cylinder, Numer. Heat Transfer 9 (1986) 591–604.
[9] T.S. Lee, Numerical Experiments with laminar fluid convection between concentric and eccentric heated rotating cylinder, Numer. Heat Transfer 7 (1984) 77–87.
[10] J.S. Yoo, Mixed convection of air between two horizontal concentric cylinders with a cooler rotating outer cylinder, Int. J. Heat Mass Transfer 41 (1998) 293–302.
[11] J.S. Yoo, Natural convection in a narrow horizontal cylindrical annulus, $Pr < 0.3$, Int. J. Heat Mass Transfer 41 (1998) 3055–3073.
[12] J.S. Yoo, Transition and multiplicity of flows in natural convection in a narrow horizontal cylindrical annulus: $Pr = 0.4$, Int. J. Heat Mass Transfer 42 (1999) 709–722.
[13] J.S. Yoo, Prandtl number effect on bifurcation and dual solution in natural convection in a horizontal annulus, Int. J. Heat Mass Transfer 42 (1999) 3279–3290.
[14] J.S. Yoo, Dual free convective flow in a horizontal annulus with a constant heat flux wall, Int. J. Heat Mass Transfer 46 (2003) 293–302.
[15] M.A. Teamah, M.M. Sorour, R.A. Saleh, Mixed convection between two horizontal concentric cylinders when the cooled outer cylinder is rotating, Alexandria Eng. J. 44 (2005) 293–302.
[16] K.F. Shi, W.Q. Lu, Numerical simulation of double-diffusive convection with cross gradients, J. Eng. Thermophys. 26 (2) (2005) 328–330.
[17] K.F. Shi, W.Q. Lu, Time evolution of double-diffusive convection in a vertical cylinder with radial temperature and axial solutal gradients, Int. J. Heat Mass Transfer 49 (6) (2006) 995–1003.
[18] H.J. Sung, W.K. Cho, J.M. Hyun, Double-diffusive convection in a rotating annulus with horizontal temperature and vertical solutal gradients, Int. J. Heat Mass Transfer 36 (1993) 3773–3782.
[19] J. Lee, S.H. Kang, Y.S. Son, Experimental study of double-diffusive convection in a rotating annulus with lateral heating, Int. J. Heat Mass Transfer 42 (1999) 821–832.
[20] J. Lee, S.H. Kang, Y.S. Son, Numerical study of multi-layered flow regime in double-diffusive convection in a rotating annulus with lateral heating, Numer. Heat Transfer: Part A 38 (2000) 467–489.
[21] A.M. Al-Amiri, K.M. Khanafer, Numerical simulation of double diffusive mixed convection within a rotating horizontal annulus, Int. J. Thermal Sci. 45 (2006) 567–578.
[22] S.V. Patankar, Numerical Heat Transfer and Fluid Flow, McGraw-Hill, New York, 1980.